PowerFactory-Python based assessment of frequency and transient stability in power systems dominated by power electronic interfaced generation

Jorge Mola-Jimenez, Jose L. Rueda*, Arcadio Perilla,
Wang Da, Peter Palensky and, Mart van der Meijden†
Faculty of Electrical Engineering, Mathematics and Computer Science
Delft University of Technology, Delft, Netherlands
† TenneT TSO B.V, Arnhem, Netherlands
* J.L.RuedaTorres@tudelft.nl

***Abstract*—The deployment of variable renewable energy based power plants is increasing all over the world, however, unlike conventional power plants these are mostly connected to the grid via power electronic interfaces. High penetration of power electronic interfaced generation (PEIG) has an important impact on the inertia of the system, which is of major concern for frequency and large disturbance rotor angle (transient) stability. Therefore, it is desirable to study the effectiveness of widely used approaches to assess the stability of a system with high penetration of PEIG. This paper concerns with the modelling and control aspects of a power system for the evaluation of the most widely used metrics (indicators) to assess the dynamics of the power system related to frequency and rotor angle stability. The functionalities of Python are used to automate the generation of operational scenarios, the execution of time domain simulations, and the extraction of signal records to compute the aforesaid indicators. The paper also provides a discussion about possible improvements in the application of these indicators in monitoring tasks.**

***Index Terms*—frequency stability, key performance indicators, power electronics interfaced generation, power system dynamics, transient stability, wind power.**

I. Introduction

The electrical power grid is a massive and complex system with a non-linear dynamic performance, which can be excited by different types of disturbances, and can manifest in different forms of stability phenomena [1].

The future power system has in its dynamic behaviour the main challenge to properly expand with the massive inclusion of power electronic interfaced generation (PEIG) [2], which due to their output variability, and decoupling from the transmission network, impacts the overall stability of the system. Thus, motivating a revision of the approaches used in monitoring and control tasks.

Displacement of conventional power plants with synchronous generator by PEIG lowers the inertia, which decreases the robustness of the system against disturbances, and is reflected in higher excursions of frequency [3] and machine rotor angles [4]. Hence, there is a renewed interest in evaluating the approaches used to estimate the proximity of the system to frequency or transient unstable condition. Constant monitoring of systems parameters is vital to prevent widespread disruptions and system collapse.

Several researches have proposed numerous options of early detection of stability issues, which employ computational intelligence tools to predict the value of a selected stability indicator. Such approaches have been developed and tested in systems dominated by synchronous generation [5], [6]. Nevertheless, further research effort is needed to improve the accuracy and reliably prediction (or alternatively classification) throughout changing operating conditions (load level, generation dispatch, and topology). This is specially critical in systems with reduced inertia and short circuit capacity.

This paper provides an evaluation of the suitability of selected and widely used indicators in both, industry and academia, for frequency and transient stability assessment in systems with high penetration of PEIG. The study is conducted on a three area system, original introduced in [7], and modified to have high penetration of wind power plants (62% of the total installed capacity), to measure the distance to frequency and transient instability in power systems with high penetration levels of PEIG.

II. A review on stability indicators

The lack of ineffective participation of PEIG in the frequency containment period, rises a concern with the assessment of the frequency performance in the mentioned interval, in which the lack of assistance by PEIG can result in large frequency gradient [8]. Therefore, the selected frequency indicators are related to this period. For rotor angle stability assessment, Power angle-based stability margin indicator and COI-referred rotor angles TSI (transient stability indicator) are considered.

A. Frequency performance indicators

1) Rate Of Change Of Frequency (ROCOF): This metric corresponds to the frequency gradient after an imbalance event of active power generation and load demand [9]. The frequency starts deviating from rated value as an immediate result of a generation loss.

The ROCOF is defined analytically as shown in (1) and for the computation of the frequency derivative, some current practice is to compute the ROCOF in two ways: the first one is with the use of the approximation taken from [10] given by (2) for qualitative assessment of the frequency performance within the time window of the system inertial response and, the second is by computing the slope of the frequency decrease in a fixed time window of 0.5s after a disturbance.

$$RoCoF = \frac{df}{dt} \tag{1}$$

$$RoCoF = \frac{f \times \Delta P}{2(E_{sys} - E_{lost})} \tag{2}$$

where ΔP is the MWs lost (i.e power deficit), f is the system frequency, E_{sys} is the system kinetic energy in MWs, E_{lost} is the kinetic energy lost in MWs.

The relevance of the ROCOF lays on the data acquisition speed of the equipments associated to frequency measurement and protection, for which the frequency shouldn't change faster than these equipments can detect.

B. Transient performance indicators

1) Power angle-based stability margin: This indicator shows a percentage value about the maximum angular deviation between any two synchronous machines within the electrical system.

This indicator is defined as follows:

$$Margin = \frac{360^\circ - \delta_{\max}}{360^\circ + \delta_{\max}} \times 100\% \tag{3}$$

where $\delta_{\max}$ is the maximum angle separation of any two generators of the system at the same time in the post fault response [11].

The relevance of this indicator is on the information about the possible islanding because it monitors the rotor angles in the system. The loss of synchronism and the activation of out-of-step relays are reflected in lower values of this metric. The range of δ is $[-180^\circ, +180^\circ]$[1], for which a value of $Margin \cong 33.3\%$ means a total separation between areas of 180°.

2) COI-referred rotor-angles TSI: This indicator is based on equivalent inertia values as a represetation of the total inertia of each area and for the entire system [12], and it is defined as shown in (4).

$$TSI_k = \begin{cases} 0 & if \quad \left|\delta_k^{COI_{system}}\right| < \delta_{\lim} \\ \frac{\left|\delta_k^{COI_{system}}\right| - \delta_{\lim}}{\pi - \delta_{\lim}} & if \quad \delta_{\lim} \leq \left|\delta_k^{COI_{system}}\right| \leq \pi \\ 1 & if \quad \left|\delta_k^{COI_{system}}\right| > \pi \end{cases} \tag{4}$$

where

$$\delta_j^{COI_{system}} = \delta_{COI_j} - \delta_{COI_{system}} \tag{5}$$

[1]In this work the domain of the rotor angle δ is $[-180^\circ, 180^\circ]$, for which the range of the $Margin$ metric is $0 - 100\%$.

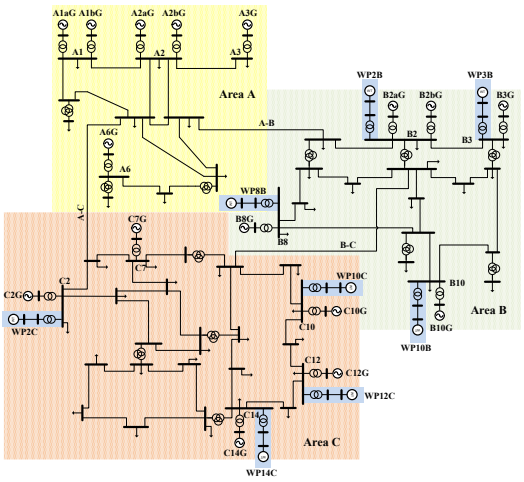

Figure 1: PST 16 benchmark system. Taken from [13] and modified to have 62% installed capacity of PEIG.

The terms δ_{COI_j} and $\delta_{COI_{system}}$ are the equivalent rotor angles of area j and the entire system. In literature these equivalences are known as Center Of Inertia or COI. To compute these values, (6) is used.

$$\begin{aligned} \delta_{COI_{system}} &= \frac{1}{H_T} \sum_{j=1}^{r} H_j \delta_{COI_j} \\ H_T &= \sum_{j=1}^{r} H_j \end{aligned} \tag{6}$$

where H_j is the equivalent inertia of area j and H_T is the overall inertia of the system.

Typical value for δ_{lim} is $\pi/3$ [12], which is the maximum allowed angle determined by steady-state constraint.

III. Modelling Approach

A. Modified PST16 benchmark system

The 16 PST benchmark system shown in Fig. 1 is used for both Frequency and rotor angle stability studies using the same simulation platform (DIgSILENT PowerFactory).

The grid consists of three strongly meshed areas, 66 buses, 16 generators, 28 transformers and 51 transmission lines, of which 3 are considered as weak transmission lines because of their length (200km transmission lines); such lines are used to interconnect the areas. The loads are concentrated in area C and power is transferred from areas A and B to area C through two long tie-lines. The generation and load demand are distributed as shown in Table I.

TABLE I: Winter peak load and generation distribution in PST 16 benchmark system.

	Load (MW)	**Generation (MW)**
Area A	2000	4840
Area B	6100	5651.71
Area C	7465	5450.00
Total	15565	15941.71

The system considers 5 hydro power units, 7 thermal (coal) and 4 nuclear. The last two are located in areas B and C. The wind parks installations are located on these two areas.

Synchronous generators are modelled using the built-in objects *ElmSym* and *TypSym* of PowerFactory, based on the sixth order model. The excitation system used corresponds to the modified IEEE type 1 model; while the governor systems differs from the technology of generation unit, i.e., whether the prime mover is steam or water, and the implemented models are TGOV1 and HYTGOV1, respectively. Detailed information is available in [13].

B. Wind turbine model

The wind turbine model was built based on the standard IEC 61400-27 series from [14]. In the mentioned standard, the modular structure of the WT models can be done using Type 1 (1A or AB), Type 2, Type 3 (3A or 3B) or Type 4 (4A or 4B) wind turbines (check [14] for detailed information). However, for sake of implementation in PowerFactory, in this development the type 4 WTs has the same aerodynamic model like type 3 and its simplified active power control model was replaced by a more detailed one of type 3. The previous statement implies that the only difference between both WT types is the generator system block, therefore, it can be selected between WT type 3A, 3B or 4 under this block. Because of this, only one model is used to represent both turbines, being possible to change the type of the wind turbine (Type 3A, 3B or 4) by changing the generator system. As it can be seen in Fig. 1, there are eight wind farms of which seven are type 4 (representing 8899.45MW of installed capacity) and one is type 3 (954MW of installed capacity). Fig. 2 can be used as a reference for the overall structure of the WT control scheme.

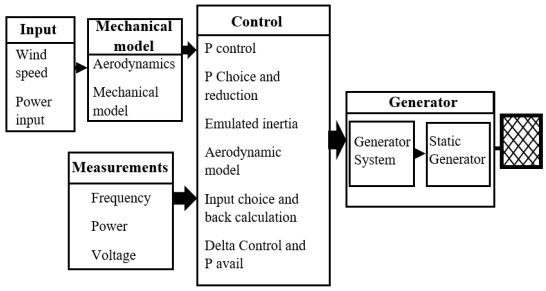

Figure 2: Block diagram showing the overall structure of WT controller.

C. Generated operating conditions and disturbances

The wind parks were installed with the same capacity of the synchronous generators on their point of common coupling (PCC), with the intention to study a change in the power share in the system but also to study when a wind park completely replaces a synchronous generator without modifying the overall power generation. It is worth to clarify that such situation (wind park installed in the same node of a conventional power plant) may not happen in reality, but given the fact that the system is not a detailed representation of a real system, adding a few lines and transformers to recreate a new generation addition, will not change significantly the simulation outcomes.

There are three load demand cases taken into account: Winter (100%), Spring (80%) and Summer (60%); where the 100% represents 15565MW as shown in Table I. For each case several dispatch scenarios are studied, where the main variation is done in the power share between synchronous and wind generation, i.e., under each season several simulations are ran where only the power share is changed (the power flow direction is not altered).

In each simulation case a set of operating scenarios are designed such that the wind generation progressively takes over the synchronous one, specifically, over the thermal and nuclear units in areas B and C. Including the removal from the system of a whole thermal power plant.

For assessment of ROCOF, the normative contingency for continental Europe, according to [9], is the generator outage of the two biggest generation units in one busbar. However, this doesn't apply directly to a test system like the one being used in this paper, because such event exacerbate the instability of the system and prevents unveiling interesting results that are found at the edge of instability. For this reason, the biggest conventional generation unit (with 1000 MW represents 6.3% of total power) is considered as the most critical generator outage for this system.

On the other hand, for transient stability studies the most critical contingency to be applied is a short circuit in the tie line A-C with a Fault Clearing Time of 152ms, which is shorter than the Critical Clearing Time (which was found to be 156ms). The criticality of the outage was corroborated based on steady-state analysis of the system in N-1 case, where the Power Flow Index, defined in [15] as shown in (7), is utilized to find the line where a short circuit causes the biggest impact in the system.

$$\begin{aligned} PFI = \frac{1}{NL}\sum_{i=1}^{NL}\left(\frac{S_{i,pos}}{S_{i,\lim}}\right)\times 100\% \quad & if, S_{i,pos} < S_{i,\lim} \\ PFI = 100\% \quad & if, S_{i,pos} > S_{i,\lim} \end{aligned} \tag{7}$$

where $S_{i,pos}$ is the actual apparent power flow through the i^{th} line, and $S_{i,\lim}$ is the apparent power flow limit in MVA.

The tie line A-C caused the biggest post-contingency PFI (when the system is highly vulnerable to transient instability) in the system which it is interpreted as the biggest electrical stress, therefore, it was selected as the worst case scenario.

IV. Simulation results

The software used for simulation is DIgSILENT PowerFactory 2016. Other software like Python 3.4, MATLAB 2016 and, Excel are also used as a complement to run simulations. The dispatch cases are established as tabulated based scenarios, using Microsoft Excel, and are dynamically read and set in PowerFactory by Python, where different events and faults are established per dispatch case. A zoom-in

into the procedural blocks for the simulation process can be conceived schematically in Fig. 3, where the data extraction block, which was programmed in Python, is broke down into detailed steps. In the figure can be seen that branch outages were automated, while the event was always the same (one synchronous generator outage).

Numerical experiments were performed on a Dell Latitude E7450 personal computer with an Inter(R) Core (TM) i7-4600U CPU, 2.10 GHz processing speed, and 8 GB RAM.

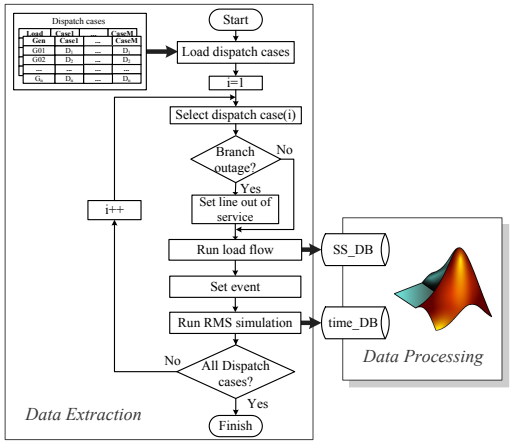

Figure 3: Flow diagram for data extraction in PowerFactory and Python. *SS_DB* refers to Steady State results data base, while *time_DB* refers to time domain results data base.

A. Effect of increased wind generation on frequency stability performance

Different generation profiles are configured to run simulations and compute the ROCOF when the PEIG gradually replaces the conventional units. The simulations are such that: first the wind generation gradually replaces conventional units in the area B, while area A and C remain untouched; then the wind generation gradually replaces conventional units in the area C, while area A and B remain untouched; and finally the wind generation gradually replaces conventional units in both areas B and C.

At every dispatch profile the power output from synchronous generators gets reduced and the wind turbine increases. Also, a complementary information to the dispatch scenarios, already provided, is the following information that completes the environment for getting the system profile: Line A-C is set out of service (same simulation case is ran twice, one with no topological changes and one with line A-C out of service). The event is a generator outage representing 6.3% of the total generation. The generator name is A1bG (see Fig. 1). Winter (as shown in Table I), Spring (taken as 80% of Winter) and Summer (taken as 60% of Winter) peak load demands are configured.

The results of all simulation cases described above are shown in Fig. 4, where it is observable that the trend of ROCOF is such that the values are higher when the inertia is low,

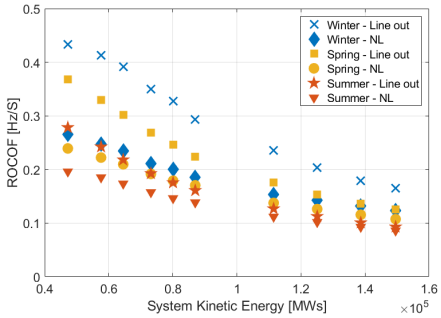

Figure 4: ROCOF vs Systems inertia for different dispatch configurations. The subscript *"NL"* refers to simulation cases with *"No line out"*, while *"Line out"* refers simulation cases where the line *A-C* was out of service.

which happens when wind generation replaces synchronous generators, this means that, as it is well known, there is a clear relation between the frequency response and the overall system inertia, as stated in (2).

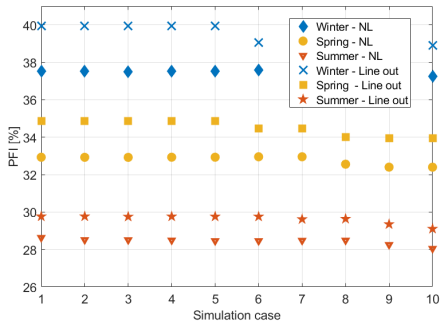

Figure 5: Power Flow Index (PFI) for sensitivity analysis. This figure is complementary with Fig. 4.

However, when the system topology changes (e.g., a crucial line outage) and/or the load demand varies such that the electrical stress of the system also varies, the frequency tends to respond more abruptly (although with the same trend), which is observed in dotted lines in Fig. 4 even though the inertia is the same. This figure shows all simulations plotted together and it can be read different values of ROCOF for the same inertia level depending on the loading level and topology of the system.

The electrical stress of the system for winter is higher than spring and higher than summer, which can be captured with the PFI, shown in Fig. 5; however, these values get even higher when a line outage is done (as also does the ROCOF), i.e., the increasing of the PFI, caused in this test system by a tie line outage or the load demand variation, reflects that the electrical stress in the system has increased and it results in higher values of ROCOF, even when there is no change in the system inertia nor in active power imbalance (same generator outage).

Fig. 4 and Fig. 5 reveal a dependence of the ROCOF not only on systems inertia but in systems loading levels as well. From such figures it could be suggested that an overload

metric, like PFI, on each case could work as an off-set value for ROCOF. Further investigation is needed to find a more suitable metric to associate the loading/stress level of the system to the value of ROCOF for a given inertia level. Such metric shall take into account the properties of the load (e.g. voltage/frequency dependency).

B. Effect of increased wind generation on transient stability performance

Different operating conditions are also generated to evaluate the transient stability performance to have a better and improved understanding about the sources of possible unstable operating conditions. The main factor to be modified over simulation cases is the level of penetration of wind power generation.

The simulations are such that: First the synchronous generation units in area B are being gradually replaced by wind parks while areas A and C remain untouched (6 dispatch cases); then the synchronous generation units in area C are being gradually replaced by wind parks while areas A and B remain untouched (4 dispatch cases).

In these set of simulation cases the area B doesn't return to zero wind generation, instead it remains at 100% while area C increases its wind power share, which implies that the decrease of synchronous generators is continuous along each simulation case. The event is as described in section III-C (short-circuit in line tie A-C with fault clearing time of 152ms).

The results are shown by comparing the three seasons in one picture, which are the product of the sensitivity analysis with respect three different loading levels. For the indicator COI-Referred rotor-angle TSI, Fig. 6 shows the results for each simulation case. The definition of this metric is such that the closer the results are to 1 p.u, the worst the transient stability of the system.

From Fig. 6 some interesting results are observed:

1) Due to the fact that the values of this indicator are predominantly around 0.5 p.u, with very low variation, it doesn't reveal approximations to dangerous values (but instead jumps from 0.5 p.u to unstable). It is not possible to find at which operating condition the system is critically stable.
2) The transient stability of the system varies greatly depending on the loadability level (seen in the figure as Winter, Spring and Summer), for which the system load demand is a crucial aspect to consider in a regular basis, as it affects the stability of the system.
3) This indicator properly marks an unstable operating condition, so it can be used to classify the stability (as stable or unstable) but not to assess the distance and tendency to move to unstable condition (e.g. as a consequence of decrease in power share from synchronous generators due to the increase of wind power share).

Despite the proper calling of unstable situation, this indicator lacks the information to measure the distance and tendency to move to unstable condition. This fact is evidenced in cases 30% and 36% of total wind generation from Fig. 6 for Spring,

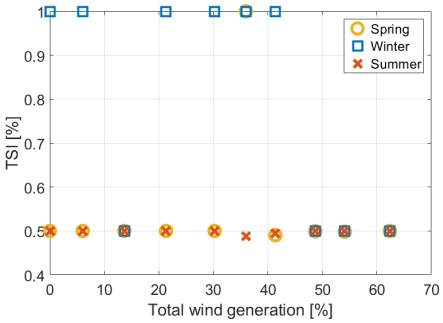

Figure 6: Results of COI-Referred rotor-angle TSI computations under the aforementioned batch of simulations.

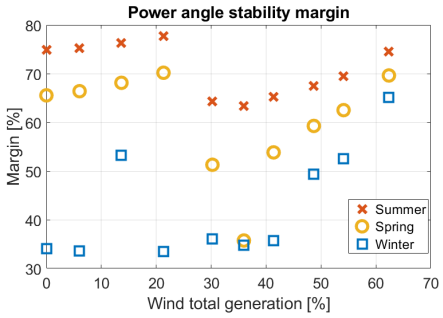

Figure 7: Results of margin index computations.

where the wind power share is relatively close between each other and the indicator didn't show any type of dangerous values (but still stable), and instead, it jumped abruptly to reflect the occurrence of instability.

Fig. 7 shows the results of the second indicator for transient stability, the power angle based stability margin (from now on will be referred as *margin*) for each simulation case. The definition of this metric is such that the closer the results to 30%, the bigger the angular separation and thus, it reflects synchronous generators approaching to a loss of synchronism (see section II-B).

From Fig. 7, some interesting results are observed:

1) After 36% of total wind generation, when PEIG is increased in area C, there is a trend of the system to become more stable, which means that while more wind generation is present, more transient stable the system is. This is due to the fact that more wind power generation is used to cover locally the demand (Area C is predominantly consuming), whereas less power transfer occurs in the tie lines and the synchronous generators of the system have reduced output power (active and reactive). It is important not to draw general conclusions based on the mentioned value for PEIG, since it is also observed that a clear relationship between the margin index and the penetration level of PEIG (or equivalently the remaining share from synch. generation) cannot be defined. This emphasizes the non-linear nature of transient stability.

2) This metric is more descriptive than the *COI-referred rotor-angle TSI*, since it utilizes almost the entire range of the possible results. This is important because intermediate conditions (stable but closest to instability) can be read from here.
3) This metric shows more clearly the effect of the load demand (Winter, Spring, Summer) on the stability of the system.

A $Margin$ of 33% represents an angular difference between any two generators of 180°, 56% a difference of 100°, while higher values (above 70%) represent shorter and safer angular differences between generators. This indicator properly displays the values that are taken as dangerous, since a value of 50% does not trigger any out-of-step relay, but might cause an islanding status in the system.

V. Outlook of improvements for tools to monitor proximity to instability in the control room

From the analysed cases in the previous section it is valid to declare that most of the current indicators for frequency and transient stability assessment can be valid when studying high penetration of PEIG. However, these indicators are the result of measurements of physical phenomena like the lowest frequency value, or the speed of frequency decrease, or the maximum angular deviation between generators. ROCOF and Margin are single values of instantaneous measurements without further information about future behaviour of the system.

In order to measure a possible distance to instability it is necessary to develop new methodologies that use advanced platforms like WAMS to assess the distance to instability and the impact of operational changes on a regular basis (e.g. intra-hour and real-time applications). Reliable and accurate estimation of system inertia from PMU data is crucial for this purpose.

VI. Conclusions

The modelling of an electrical power system with high penetration of power electronics interfaced generation is developed and exploited using the simulation capabilities of DIgSILENT PowerFactory, together with Python for automated execution of such simulations. The results of the multiple cases ran in this work show that, for frequency stability, the current practices might have a level of dependency on the overloading level of the system for the frequency stability assessment in the containment phase. This work makes a call to incorporate this information in the calculations to estimate a possible distance to instability. On the other hand, for rotor-angle stability studies, the current practices are found to be appropriate to monitor the behaviour of the system in real time applications, although there are limitations on some popular metrics, like the COI-referred rotor-angle TSI, which is found to be more suitable to assess and help in classifying the stability status.

VII. Acknowledgement


This project has received funding from the European Union's Horizon 2020 research and innovation programme under grant agreement No 691800

This paper reflects only the authors' views and the European Commission is not responsible for any use that may be made of the information it contains.

References

[1] P. Kundur, J. Paserba, V. Ajjarapu, G. Andersson, A. Bose, C. Canizares, N. Hatziargyriou, D. Hill, A. Stankovic, C. Taylor, T. V. Cutsem, and V. Vittal, "Definition and classification of power system stability ieee/cigre joint task force on stability terms and definitions," *IEEE Transactions on Power Systems*, vol. 19, no. 3, pp. 1387–1401, Aug 2004.

[2] R. Eichler, C. O. Heyde, and B. O. Stottok, *Composite Approach for the Early Detection, Assessment, and Visualization of the Risk of Instability in the Control of Smart Transmission Grids*. Cham: Springer International Publishing, 2014, pp. 97–122.

[3] J. Eto et al., *Use of Frequency Response Metrics to Assess the Planning and Operating Requirements for Reliable Integration of Variable Renewable Generation.* [online] Ernest Orlando Lawrence Berkeley National Laboratory, pp.1-141. Available at: https://www.ferc.gov/industries/electric/indus-act/reliability/frequencyresponsemetrics-report.pdf [Accessed 1 Oct. 2017].

[4] F. Shewarega, I. Erlich, and J. L. Rueda, "Impact of large offshore wind farms on power system transient stability," in *2009 IEEE/PES Power Systems Conference and Exposition*, March 2009, pp. 1–8.

[5] X. He, R. C. Qiu, Q. Ai, L. Chu, X. Xu, and Z. Ling, "Designing for situation awareness of future power grids: An indicator system based on linear eigenvalue statistics of large random matrices," *IEEE Access*, vol. 4, pp. 3557–3568, 2016.

[6] T. Wang, T. Bi, H. Wang, and J. Liu, "Decision tree based online stability assessment scheme for power systems with renewable generations," *CSEE Journal of Power and Energy Systems*, vol. 1, no. 2, pp. 53–61, June 2015.

[7] S. P. Teeuwsen, I. Erlich, M. A. El-Sharkawi, and U. Bachmann, "Genetic algorithm and decision tree-based oscillatory stability assessment," *IEEE Transactions on Power Systems*, vol. 21, no. 2, pp. 746–753, May 2006.

[8] MIGRATE H2020 Project, "Deliverable 1.1: Report on systemic issues," [online] TENNET GmbH, pp.1-137. Available at: https://www.h2020-migrate.eu/downloads.html [Accessed 1 Oct. 2017].

[9] "Frequency stability evaluation criteria for the synchronous zone of continental europe," ENTSO-E, Brussels, Belgium, Tech. Rep., 2016.

[10] I. Dudurych, M. Burke, L. Fisher, M. Eager, and K. Kelly, Operational Security Challenges and Tools for a Synchronous Power System with High Penetration of Non-conventional Sources, CIGRE 2016 Session, C2-116, 2016.

[11] Powertech Labs Inc., "Transient security assessment tool: User manual," Surrey, British Columbia, Canada, Tech. Rep., 2011. [Online] Available at: https://eva.fing.edu.uy/pluginfile.php/71802/mod_resource/content/1/TSAT_User_Manual.pdf [Accessed 1 Oct. 2017].

[12] J. C. Cepeda, J. L. Rueda, D. G. Colom, and D. E. Echeverra, "Real-time transient stability assessment based on centre-of-inertia estimation from phasor measurement unit records," *IET Generation, Transmission Distribution*, vol. 8, no. 8, pp. 1363–1376, 2014.

[13] J. L. Rueda, J. C. Cepeda, I. Erlich, A. W. Korai, and F. M. Gonzalez-Longatt, *Probabilistic Approach for Risk Evaluation of Oscillatory Stability in Power Systems*. Cham: Springer International Publishing, 2014, pp. 249–266.

[14] *Electrical simulation models – wind turbines,* IEC standard 61400-27-1, 2015.

[15] J. M. G. Alvarez and P. E. Mercado, "Online inference of the dynamic security level of power systems using fuzzy techniques," *IEEE Transactions on Power Systems*, vol. 22, no. 2, pp. 717–726, May 2007.